Engineering Structures 32 (2010) 2776–2792

Contents lists available at ScienceDirect

Engineering Structures

journal homepage: www.elsevier.com/locate/engstruct

Spectral shape-based assessment of SDOF nonlinear response to real, adjusted and artificial accelerograms

Iunio Iervolino, Flavia De Luca *, Edoardo Cosenza

Dipartimento di Ingegneria Strutturale, Università degli Studi di Napoli Federico II, Naples, Italy

ARTICLE INFO

Article history:
Received 1 December 2009
Received in revised form
4 April 2010
Accepted 28 April 2010
Available online 3 June 2010

Keywords:
Spectral matching
Real records
Scaling
Artificial accelerograms
RSPMatch 2005

ABSTRACT

The simple study discussed in this paper compared different procedures to obtain sets of spectral matching accelerograms for nonlinear dynamic analysis of structures in terms of inelastic seismic response. Six classes of records were considered: original (unscaled) real records, real records moderately linearly scaled, real records significantly linearly scaled, real records adjusted by wavelets, and artificial accelerograms generated by two different procedures. The study is spectral shape-based; that is, all the considered sets of records, generated or selected, match individually (artificial and adjusted) or on average (real records) the same design spectrum for a case-study site in Italy. This is because spectral compatibility is the main criterion required for seismic input by international codes.

Three kinds of single degree of freedom (SDOF) system, non-degrading and non-evolutionary, non-degrading and evolutionary, and both degrading and evolutionary, were used to evaluate the nonlinear response to the compared records. Demand spectra in term of peak and cyclic responses were derived for different strength reduction factors.

Results of the analysis show that artificial or adjusted accelerograms may underestimate, in some cases, and at high nonlinearity levels, the displacement response, if compared to original real records, which are considered as a benchmark herein. However, this conclusion does not seem to be statistically significant. Conversely, if the cyclic response is considered, artificial record classes show a significant overestimation of the demand, which does not show up for wavelet-adjusted records.

The two classes of linearly scaled records do not show systematic bias with respect to those unscaled for both types of response considered, which seems to confirm that amplitude scaling is a legitimate practice.

1. Introduction

Seismic assessment of structures via nonlinear dynamic analysis requires seismic input selection. Seismic codes suggest different procedures to select ground motion signals, most of those assuming spectral compatibility to the elastic design spectrum as the main criterion [1]; for example, Eurocode 8 [2] requires the average spectrum of the chosen set to be above 90% of the design spectrum in the range of periods $0.2T1$–$2T1$, where $T1$ is the fundamental period of the structure. Practitioners have several options to get input signals for their analysis: e.g., real or real manipulated records and various types of synthetic and artificial accelerograms [3]. All these options are usually acknowledged by codes which may provide additional criteria or limitations for some of them. In the Italian seismic code [4], for example, artificial records, generated by random vibration theory, should have a duration of *at least 10 s in their pseudo-stationary part*, and they cannot be used in the assessment of geotechnical structures. Synthetic records, generated by simulation of earthquakes rupture process, should refer to a characteristic scenario for the site in terms of magnitude, source-to-site distance and seismological source characteristics; finally, real records should reflect the earthquake *dominating* the hazard at the site. However, practitioners cannot always accurately characterize the seismological threat to generate synthetic signals or it is not possible to find a set of real records that fits the code requirements properly in terms of a specific hazard scenario [5].

Despite the fact that in recent decades the increasing availability of databanks of real accelerograms has determined a spreading use of real records, it may be very difficult to successfully apply code provisions to obtain code-compliant sets. In particular, provisions regarding spectral compatibility are hard to match if appropriate tools are not available [1,6]. This is why the relatively easy and fast generation of artificial records, perfectly compatible with an assigned design spectrum, is still very popular for both practice and research purposes.

* Corresponding address: Dipartimento di Ingegneria Strutturale, Università degli Studi di Napoli Federico II, via Claudio 21, 80125 Naples, Italy. Tel.: +39 0817683672; fax: +39 0817683491.
E-mail address: flavia.deluca@unina.it (F. De Luca).

0141-0296/$ – see front matter © 2010 Elsevier Ltd. All rights reserved.
doi:10.1016/j.engstruct.2010.04.047

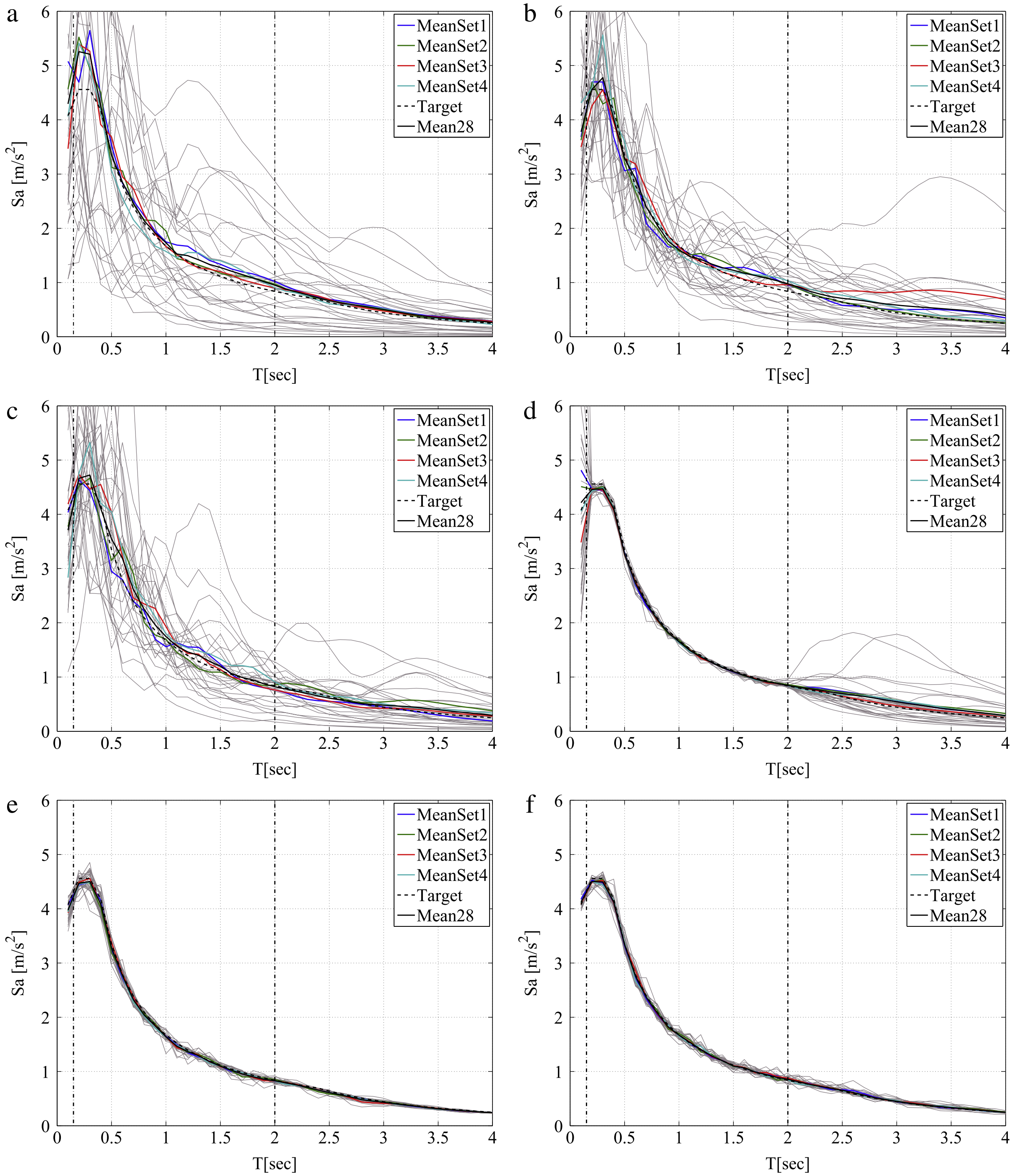

Fig. 1. URR (a), SF5 (b), SF12 (c), RSPMatch (d), Belfagor (e), and Simqke (f) acceleration elastic spectra, compared to the target spectrum.

More recently, procedures to get the spectral compatibility of real records by wavelet adjustments were proposed (e.g., [7]). This kind of manipulation is conceptually an extension of the more simple linear scaling of real records to modify (e.g., to amplify) the spectral shape to get a desired intensity level [8].

Although several studies tried to assess the *reliability* of each of these procedures (e.g., [9]), many of them do not allow to draw general conclusion. This work tries to address the spectral matching matter from the structural point of view in terms of ductility and cyclic response, having as reference a code-based design spectrum. To this aim six classes of 28 accelerograms, each of those comprised of four sets of seven, were considered: (1) unscaled real records; (2) moderately scaled real records; (3) significantly scaled real records; (4) wavelet-adjusted real records; (5) non-stationary artificial records; (6) stationary artificial records. All sets are compatible with the elastic design spectrum for a case study in southern Italy.

The seismic responses of a large number of single degree of freedom (SDOF) systems, with different backbones, hysteretic relationships, and with various strength reduction factors (R), were considered. As structural response measures, or engineering demand parameters (EDPs), the ductility normalized with respect to the strength reduction factor and the equivalent number of cycles were considered to relate the ground motions to both peak and cyclic structural demand [10,11]. Analyses aimed at comparing the differences, if any, in the EDPs associated to each class of

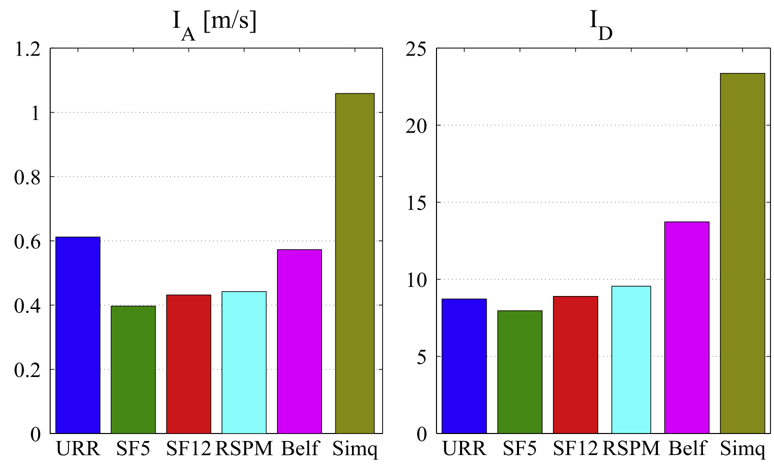

Fig. 2. Average values of I_A and I_D for the considered classes of records.

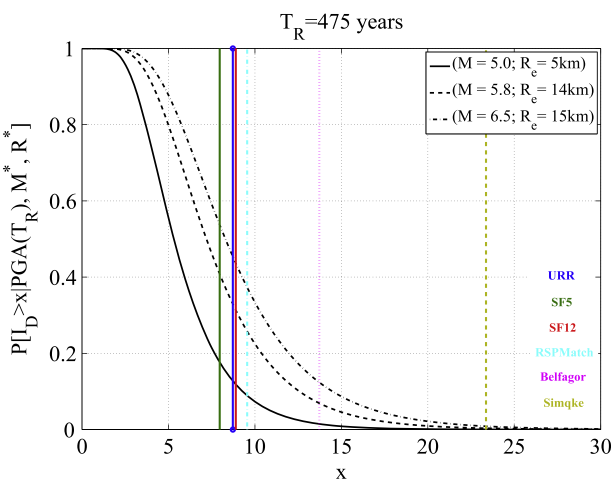

Fig. 3. Comparison between probability of exceedance of I_D conditional to the PGA value of the target elastic spectrum and I_D medium values of each record category.

records with respect to the unscaled real records, considered as a benchmark. Hypothesis tests on selected samples were also carried out to assess the statistical significance of the results found in terms of both peak response and cyclic response.

2. Record classes

All the classes of records refer to the same 5% damped elastic design spectrum evaluated according the new Italian seismic code for a case-study site in Avellino (southern Italy, latitude 40.914° N, longitude 14.780° E). The spectrum considered is that corresponding to the life-safety limit state of an ordinary construction with a nominal life of 50 years on A-type soil class, according to the Eurocode 8 classification; see [4] for details.

For each class, four spectrum compatible sets, made of seven records each, were selected (if real) or generated (if artificial) because seven is the minimum size of samples for which to consider the average structural response as the design value according, among others, to the Italian and Eurocode 8 provisions. In the following, the selection or generation processes are briefly reviewed; other information about the selection procedure can be found in [12].

2.1. URR—unscaled real records

The sets of unscaled real ground motions (URR) were selected using REXEL 2.5 (beta), software that is freely available at http://www.reluis.it/, which allows users to select combinations of seven records contained in the European Strong Motion Database (http://www.isesd.hi.is/) and the Italian Accelerometric Archive (http://itaca.mi.ingv.it/ItacaNet/), which on average match a code-based or user-defined elastic spectrum in a desired period range and with specified upper and lower bound tolerances [13]. Because REXEL can also automatically build the code spectrum for an Italian site based on its geographical coordinates, four sets of records were selected, each of those matching on average the target in the 0.15–2.0 s period range. The magnitude (moment magnitude, M_w) and source-to-site distance (epicentral, R_e) range between 5.6 and 7.8 and 0 and 35 km, respectively; the site conditions are of A type.

Because the Italian code design spectra approximate closely uniform hazard spectra provided for the Italian territory, initially the selection aimed at finding records with M_w and R_e equal to 5.8 and 14 km, respectively; i.e., to the mean from the disaggregation of peak ground acceleration (PGA) hazard at the site[1] available at http://esse1-gis.mi.ingv.it/ (official Italian hazard data). However, due to the lack of spectrum matching unscaled real record sets fitting these restraints, the M_w range had to be relaxed, obtaining average values of magnitude and distance for the class equal to 6.5 and 15 km, respectively.

In Fig. 1(a), the four sets are depicted along with the target spectrum. All the set averages are selected to be within [−10%, +30%] tolerance range with respect to the code spectrum, and in most of the compatibility interval they approximate the design spectral shape very well. To measure such an approximation, the average deviation (δ), Eq. (1), from the target spectrum may be introduced. In Eq. (1), $Sa_{o,med}(T_i)$ represents the pseudo-acceleration ordinate of the average real spectrum corresponding to the period T_i, while $Sa_s(T_i)$ is the value of the spectral ordinate of the code spectrum at the same period, and N is the number of values within the considered range of periods (0.15–2.0 s). All the URR sets have similar δ-values; in fact they are equal to 0.163 for set 1, 0.134 for set 2, 0.152 for set 3 and 0.141 for set 4. The four URR sets have no records in common and come from 17 different earthquakes, as shown in the Appendix (Table A.1).

$$\delta = \sqrt{\frac{1}{N}\sum_{i=1}^{N}\left(\frac{Sa_{o,med}(T_i) - Sa_s(T_i)}{Sa_s(T_i)}\right)^2}. \quad (1)$$

In the following, the SDOF response to various ground motion selection or generation methods will be compared referring to the

[1] More accurately, the disaggregation to be matched should be that for the hazard of the spectral ordinate at the fundamental period of the structure [14].

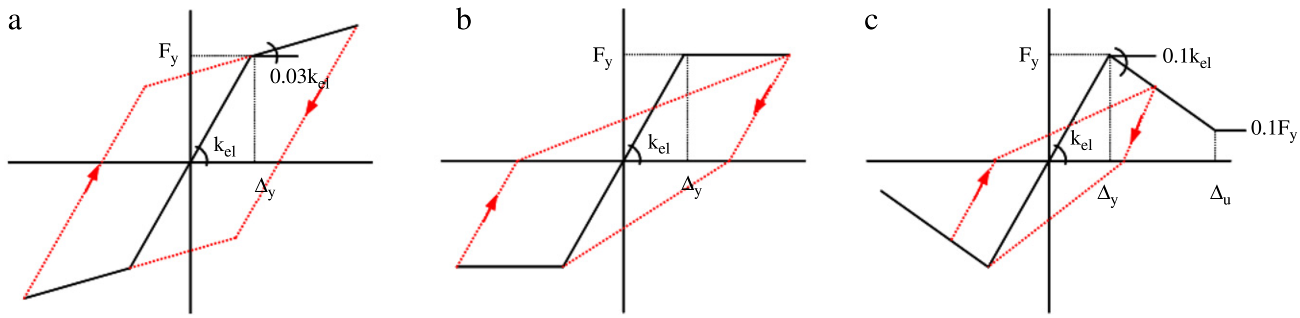

Fig. 4. EPH backbone curve (a), EPP backbone curve (b), ESD backbone curve (c).

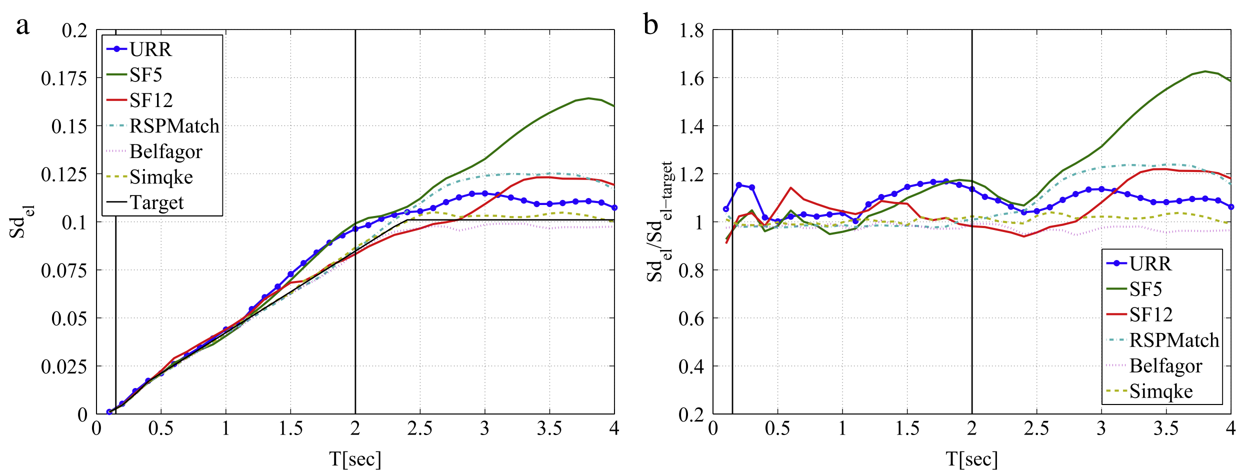

Fig. 5. Average values of elastic displacement (a) and ratio to the target spectrum (b) for the record classes.

URR response. In fact, in this kind of study it is necessary to define the "true" response (i.e., a point of comparison). Because the work herein presented is mostly aimed at comparing spectral matching in the light of code-compliant procedures, which often basically only prescribe the average spectrum of the set to match the design spectrum [1,5], the URR records are assumed as a benchmark. This means that if a systematic difference in the response from another class of records with respect to the URR class is found, this class will be considered "biased". However, this use of the *bias* term does not necessarily extend beyond this study as, in general, the URR class may be not an unbiased baseline itself, even if allowed by the code, simply because, for example, by selecting records that have a similar spectral shape, a selection bias can be created [15,16].

2.2. Scaling factor (SF)—scaled real records

REXEL also allows selecting sets of seven accelerograms compatible with the reference spectrum if linearly scaled in amplitude. In other words, before the search, the spectra are preliminarily normalized by dividing the spectral ordinates by the corresponding PGA. These non-dimensional spectra are compared to the target spectrum, also normalized. Records belonging to spectrum matching combinations found in this way require to be linearly scaled to comply with the original code spectrum. Because REXEL allows controlling the average scaling factor (SF) of the combination, two classes of four scaled records sets each, (i) SF equal to 5 and (ii) SF equal to 12, were selected from A type site class accelerograms. The intent is to compare the response to records moderately and significantly scaled.

2.2.1. SF5

In the same range of periods in which there is spectral compatibility (0.15–2 s), with the same tolerances, and in the same magnitude and distance intervals chosen for the URR sets, four sets of seven compatible accelerograms, each of those having a mean SF equal to 5, were selected; see Fig. 1(b).

The 28 records (9 records in common with the URR class) come from 15 earthquake events (10 of them are in common with the URR class), as shown in the Appendix (Table A.2).

In this case, the deviations of the sets are smaller than the URR records' deviations, as expected [1,6], being equal to 0.082 for set 1, 0.087 for set 2, 0.069 for set 3 and 0.089 for set 4.

2.2.2. SF12

Using REXEL, three sets of seven records whose mean SF was 12 were also selected, each of those matching on average the target in the 0.15–2.0 s period range. The magnitude and source-to-site distance range between 5.5 and 7.8 and 0 and 50 km, respectively. Because it was not possible to find another set with the desired characteristics via REXEL, the fourth set of seven accelerograms was "manually" selected in the same magnitude and distance ranges so that its deviation and its average scaling factor were similar to the other three software-aided selected sets; see Fig. 1(c).

These four sets have no events in common with the URR class and belong to 17 different earthquakes, as shown in the Appendix (Table A.3). In this case, the deviations of the sets are still smaller than deviations of the URR sets and comparable to deviations of the SF5 sets, being equal to 0.072, 0.078, and 0.117 for the software-selected sets and equal to 0.207 for the manually selected set, respectively.

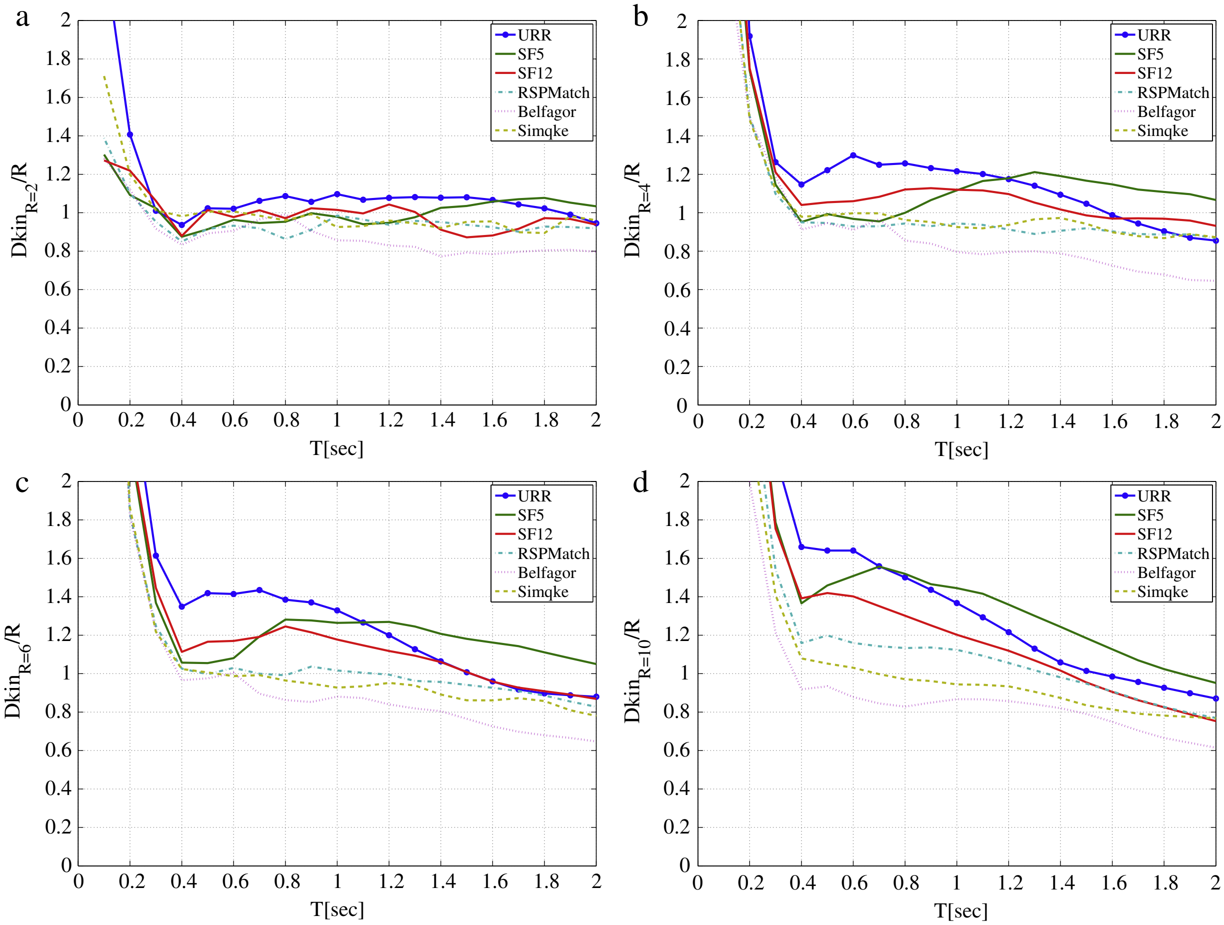

Fig. 6. Average values of ductility demand for the EPH system computed as the mean value of 28 records.

2.3. RSPMatch—wavelet adjusted records

RSPMatch2005 software[2] [17,7], was used to modify the URR accelerograms. Spectral matching software, such as RSPMatch2005, makes adjustments to recorded ground motions to provide a good match with a target response spectrum. Using spectrally matched records as an input to time-history analysis helps to reduce the variability in the seismic demand, and therefore allows fewer records to be used to obtain stable estimates of the expected response [15]. Generally, RSPMatch2005 is able to provide an excellent match of the target spectrum across a wide range of periods (and, if required, at multiple damping levels), with relatively small adjustment to the seed accelerogram. Useful guidelines and reliable selecting criteria to choose set of records suitable to be adjusted by the software can be found elsewhere (e.g., [18]).

In this case, the adjustment procedure was simply aimed at reducing the dispersion of records, in a specific period range, with respect to the target. The procedure was pursued only for the 5% damping factor in the range of periods 0.15–2.0 s in which records were already compatible on average; see Fig. 1(d).

It is worth noting that wavelet adjustment was applied in a relatively limited period range. Nevertheless, even if the matching in the 0.15–2.0 s interval produced individual spectrum modification also beyond that range (Fig. 1(d)), the average of RSPMatch class is close to the target also in the 2–4 s range.

2 Courtesy of Damian Grant, ARUP, USA.

2.4. Artificial records

Generally speaking, generation procedures for artificial accelerograms are based on the random vibration theory and the spectral matching is carried out iteratively adjusting the Fourier amplitude spectrum of each accelerogram generated [19]. In this way, spectral matching procedures are carried out in the frequency domain by the use of a power spectral density function, the selection of which is the key issue and represents the main difference between various generation procedures.

The software considered in this study generates different kinds of signal: the first one, Belfagor [20], produces non-stationary signals based on the semi-empirical method of Sabetta and Pugliese [21]; the second one, SIMQKE [22], produces stationary signals that are subsequently enveloped in a trapezoidal shape to roughly simulate the non-stationary characteristics of ground motion.

2.4.1. Belfagor sets

Belfagor (http://www.unibas.it/utenti/mucciarelli/index.html) generates non-stationary signals using variable Fourier amplitudes empirically evaluated from the Sabetta and Pugliese ground motion prediction equation [21]; in fact, the code asks for reference M_w, R_e, and soil type. Because of records' non-stationary character, these parameters influence strictly the shape of the signal even if the spectral matching procedure is based on a smooth code spectrum.

A class of 28 accelerograms was generated for the purposes of this study. The input M_w-values and R_e-values for each signal were

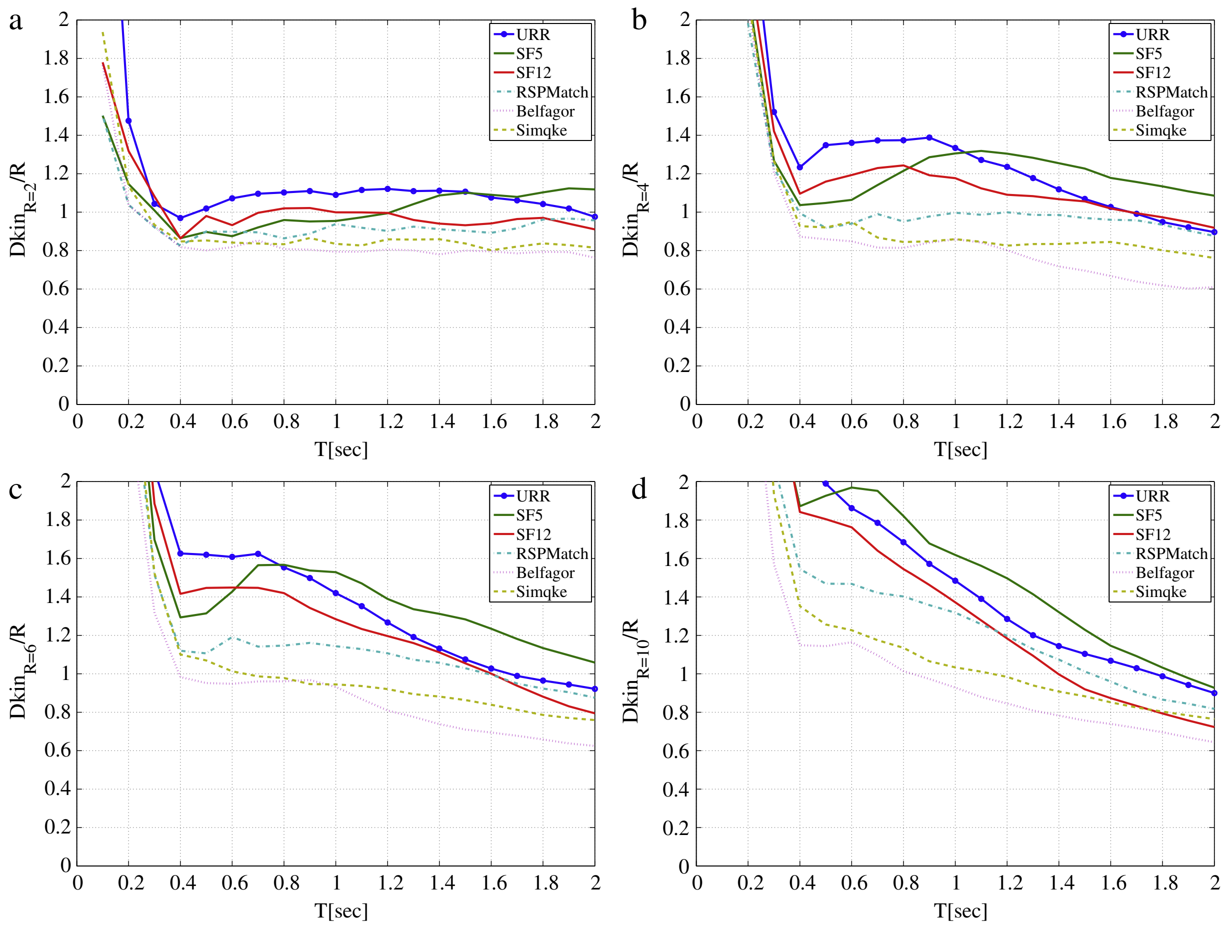

Fig. 7. Average values of ductility demand for the EPP system computed as the mean value of 28 records.

equal to those of the URR sets, and *stiff soil type*, according to [21], was assumed. All the generated records have the same duration, 21.48 s, with a 0.005 s time step (default values of Belfagor). The duration is slightly lower than the minimum prescribed by the Italian code for artificial records (25 s); however, this 15% difference is not believed to affect the results (see also Section 2.5).

Although not strictly necessary for the purposes of this study, the accelerograms were randomly arranged in four sets of seven, consistently with the other classes; see Fig. 1(e).

2.4.2. Simqke sets

A second class of artificial records was generated by Simqke (http://bsing.ing.unibs.it/~gelfi/software/simqke/). This is the commonly used method for generating synthetic ground motions, which are compatible with an assigned design spectrum. This method is based on the simulation of stationary processes. The matching of the target spectrum may be improved by means of an iterative procedure. Other studies evaluated the influence of iterative option in the software that was not considered in this case (e.g., [9]).

In this case, 28 records were generated in a single run of the software and subsequently they were separated into four groups of seven; see Fig. 1(f). They fully respect the Italian code's provisions in terms of duration of both stationary and non-stationary parts. In fact, as was reported previously, this software simulates non-stationary records by enveloping the signal obtained in a trapezoidal shape, and the user can choose how long to make the beginning and ending of the non-stationary part.

2.5. Integral ground motion parameters

Each accelerogram of the six classes was processed to evaluate its characteristics other than the spectral shape, in particular in terms of integral intensity measures (IMs). Average values of the Arias intensity (I_A), Eq. (2), and of the Cosenza and Manfredi index [23] (I_D), Eq. (3), computed as the average on the sample of 28 records for each class, are reported in Fig. 2. In Eqs. (2) and (3), $a(t)$ is the signal's accelerometric time-history, whose duration is equal to t_E, and PGV represents the peak ground velocity.

$$I_A = \frac{\pi}{2 \cdot g} \int_0^{t_E} a^2(t)\mathrm{d}t \tag{2}$$

$$I_D = \frac{2 \cdot g}{\pi} \frac{I_A}{PGA \cdot PGV}. \tag{3}$$

It seems that the Simqke generation process is not able to reproduce characteristic Arias intensities of real events at least if compared to the URR, SF5, and SF12 classes. Scaled real records have lower I_A-values, on average, with respect to the URR class, as well as those adjusted via RSPMatch2005. However, when passing to I_D, which is supposed to be better related than I_A to structural cyclic response expressed in terms of equivalent number of cycles [11], both scaled and unscaled real records and RSPMatch have close average values of I_D. Both classes of artificial signals display higher values of I_D, especially the Simqke accelerograms, because of the high I_A.

Also the significant duration (Sd), defined as the time interval between 5% and 95% of I_A accumulation, was computed. Table 1 reports average values of Sd for each class. Only the Simqke records show a duration clearly larger than that of the others.

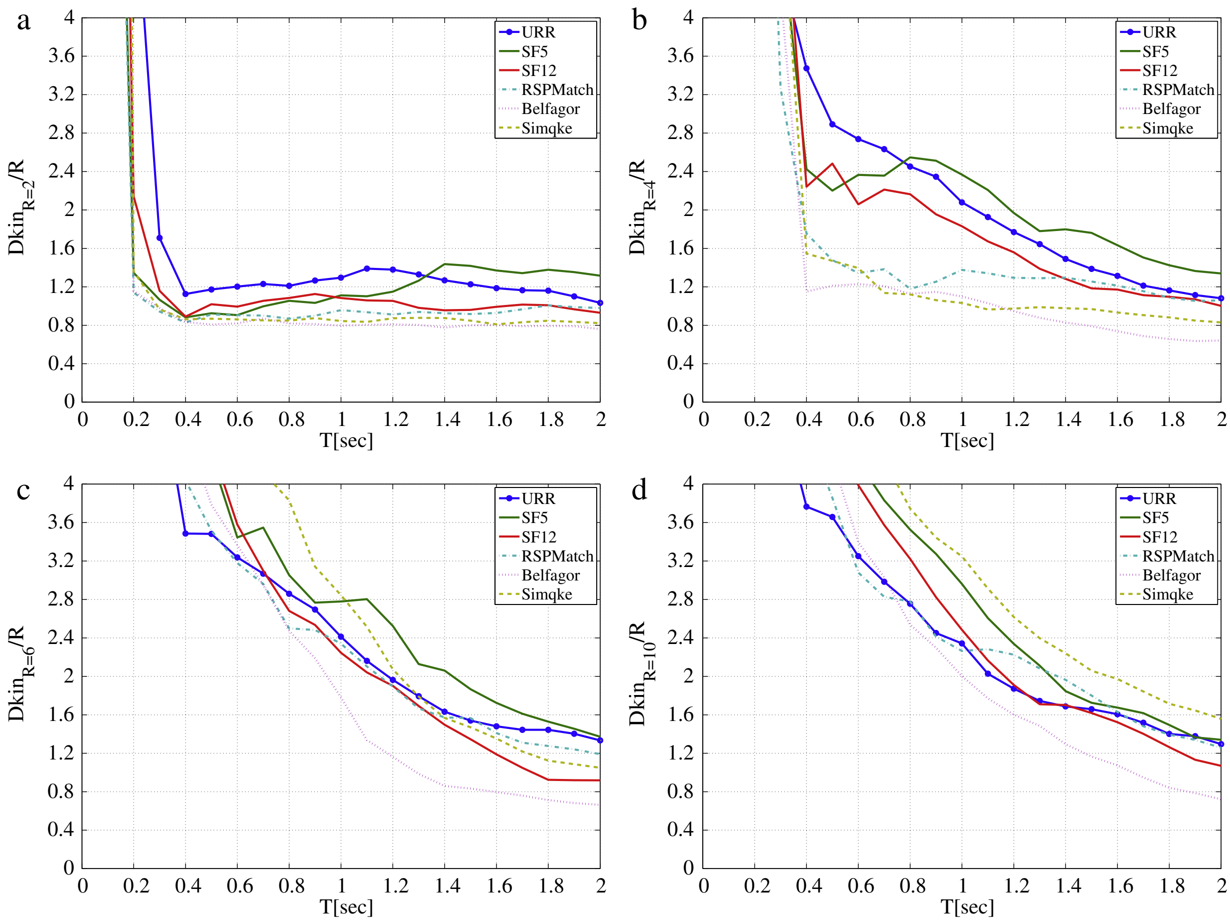

Fig. 8. Average values of ductility demand for the ESD system computed as the mean value of 28 records.

Table 1
Average values of *Sd* for the considered classes of records.

URR	SF5	SF12	RSPM	Belf	Simq
13.7 s	12.5 s	10.4 s	13.8 s	12.0 s	18.0 s

Although it was discussed how integral parameters such as I_D are good IMs for cyclic response, one may argue that the correct value to match is not necessarily that of the URR class. To investigate this, in Fig. 3 the probability of exceedance of I_D conditional to the PGA of the target spectrum is reported for three M_w–R_e pairs. The first pair chosen ($M_w = 5.0$ and $R_e = 5.0$ km) is the modal pair from disaggregation of the hazard for the design PGA at the site, and the second pair ($M_w = 5.8$ and $R_e = 14.0$ km) is the mean. For comparative purposes, a third couple of M_w and R_e ($M_w = 6.5$ and $R_e = 15.0$ km) was considered; this represents mean M_w and R_e of the URR class. The curves in Fig. 3 were obtained via *conditional hazard analysis* according to the procedure[3] described in [24,25].

The mean I_D of all the classes of records can be compared with the I_D distributions. It may be observed that the likely I_D-values given the PGA at the site are 5.3 and 7.2 as median, 3.5 and 4.7 as 16% and 8.2 and 11.1 as 84% percentile, respectively, for the mode and mean M_w and R_e from disaggregation. The URR mean M_w and R_e give 5.3, 8.3 and 12.8 as 16%, 50% and 84% percentiles, respectively.

All three complementary cumulative distributions of I_D suggest that the artificial signals are characterized by unusual integral parameters although they match the same elastic spectrum of all the other record classes.

3. SDOF systems and demand measures

All records selected for each class were used as input for nonlinear dynamic analyses applied to 240 SDOF systems. They belong to three classes of hysteretic behavior with elastic period varying from 0.1 to 2 s, sampled with a 0.1 s step. The elastic–plastic with hardening (EPH) SDOF group represents non-degrading and non-evolutionary structures. The post-yielding stiffness was assumed as 0.03 of the initial stiffness (k_{el}); see Fig. 4(a). The second group of inelastic SDOF systems has a non-degrading and evolutionary relationship; its backbone is elastic perfectly plastic (EPP) and it is characterized by a degrading stiffness; the Clough and Johnston model [26] was considered (Fig. 4(b)). The third group of inelastic SDOF systems has a softening backbone (ESD); a Takeda hysteretic rule was assumed [27]. The softening stiffness is equal to 10% of the elastic one and 10% of yielding strength was taken as the residual value. All ESD systems have ductility before reaching the residual strength, evaluated as the ratio between ultimate displacement (Δ_u) and yielding displacement (Δ_y) in the backbone curve, equal to 10. In the following, this

3 As discussed in [24,25] the conditional I_D distribution would require to account for all M_w and R_e pairs weighted by their contribution to the hazard from disaggregation and this would be the "exact" result in terms of the distribution of integral ground motion features given the design peak acceleration. However, a simplified and approximated approach may be followed using only representative pairs from the joint M_w and R_e disaggregation distribution. This approach is also used herein; different representative pairs lead to slightly different (approximated) results.

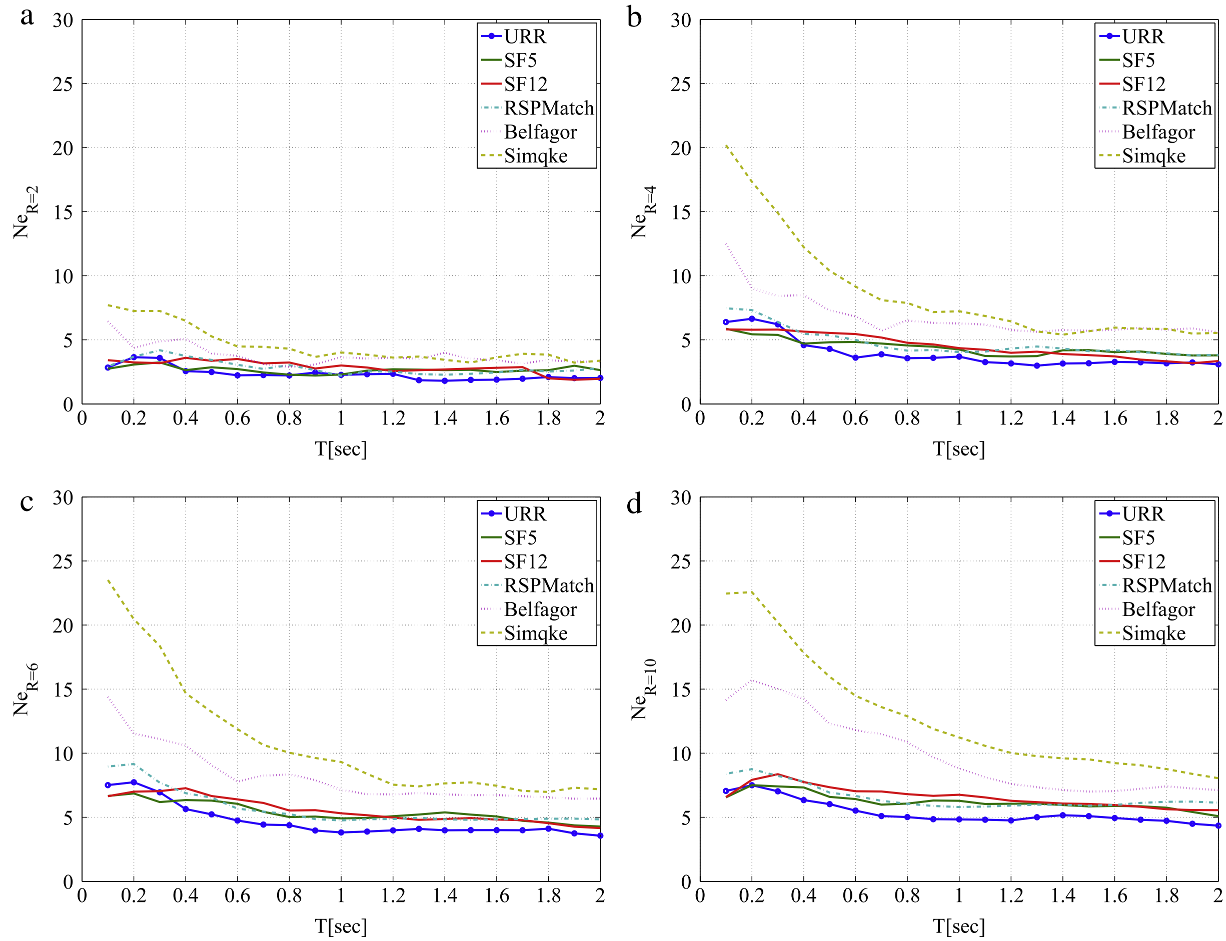

Fig. 9. Average values of the equivalent number of cycles for the EPH system computed as the mean value of 28 records.

ductility value will be called the *ductility limit*; see Fig. 4(c). In all panels of Fig. 4, F_y is the yielding strength of the SDOF system.

To have a response that ranges from mildly inelastic to severely inelastic, for all SDOF systems four strength reduction factors (R) were considered: 2, 4, 6 and 10. Note that the peak deformation experienced by an elastic structure is a ground motion specific quantity. Therefore, one can achieve the same value of R either for each record in a dataset (*constant-R approach*) or in an average sense (*constant-strength approach*), keeping constant the yielding strength. The latter was adopted in this case, to simulate the effect of different sets of accelerograms on the same structure (same F_y-value at a given oscillation period T), given the design spectrum. However, it should be emphasized that the two different approaches can lead to different conclusions, as pointed out by some authors (e.g., [28]).

3.1. Engineering demand parameters (EDPs)

The EDPs chosen were selected to investigate both the peak response and the cyclic seismic response. The displacement-based parameter is the ratio between displacement ductility and strength reduction factor (D_{kin}/R), the former evaluated as the ratio of the peak inelastic displacement ($Sd_{R=i}$) and yielding displacement, according to Eq. (4).

$$D_{kin} = \frac{Sd_{R=i}}{\Delta_y}. \quad (4)$$

The cyclic response-related parameter is the equivalent number of cycles (N_e). This latter parameter is given by the cumulative hysteretic energy (E_H), evaluated as the sum of the areas of the hysteretic cycles (not considering the contribution of viscous damping), normalized with respect to the largest cycle, evaluated as the area underneath the monotonic backbone curve from the yielding displacement to the peak inelastic displacement ($A_{plastic}$); see Eq. (5). This allows separating the ductility demand (already considered above in D_{kin}) and cyclic demand [11].

$$N_e = \frac{E_H}{A_{plastic}}. \quad (5)$$

4. Results and discussion

4.1. Elastic displacements and ratio to the target code spectrum

Elastic displacement spectra, evaluated as mean value on 28 records for each class, are compared to the target spectrum transformed from pseudo-acceleration; see Fig. 5(a).

Fig. 5(b) reports the ratio of the average spectrum of the class and the code spectrum, that is, the deviation of each class (Sd_{el}) with respect to the target spectrum ($Sd_{el-target}$), as it may help to understand the nonlinear results presented in the following. Although all classes are spectrum matching, the real record spectra show the largest deviation with respect to the target, as was anticipated. This is because real records match the target on average, while for the other three classes (adjusted and artificial records) each single record closely matches the target (see Fig. 1).

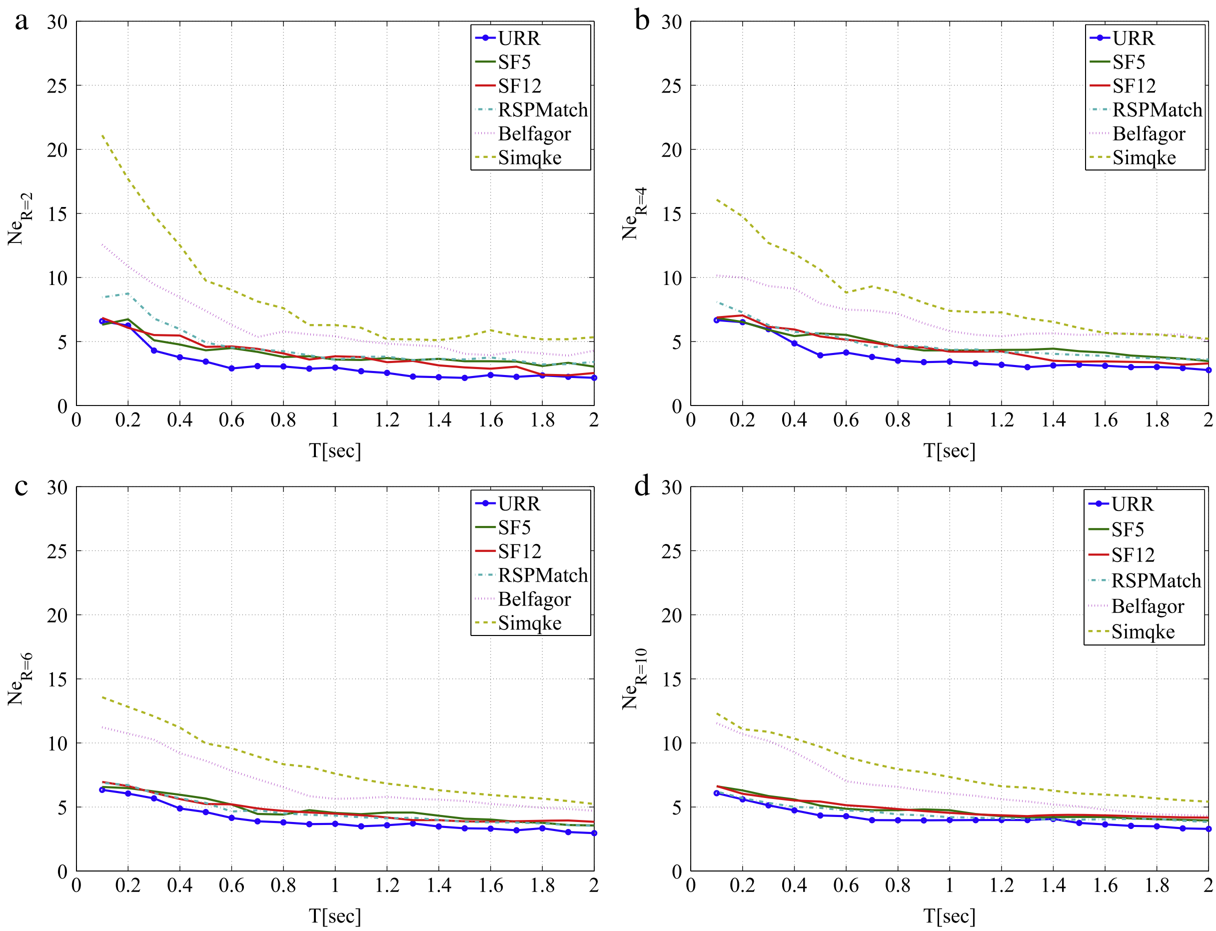

Fig. 10. Average values of the equivalent number of cycles for the EPP system computed as the mean value of 28 records.

From Fig. 5(b) it is possible to recognize that all the average spectra of the six record classes selected are above 90%, and mostly below 20%, of the target in the 0–4 s range. This renders the classes suitable, according to Eurocode 8 spectral matching provisions, for structures with a fundamental period up to 2 s.

4.2. Ductility demand

Fig. 6 shows the ductility demand normalized with respect to the different R-values investigated, referring to the EPH system. For low R, the normalized ductility seems to be similar for all six classes of records. The cases for high R-values (Fig. 6(c) and (d)) emphasize an apparent underestimation of ductility for artificial records with respect to real record classes. In particular, results for R equal to 10 show different underestimation levels for adjusted and artificial classes of records: the Belfagor class is followed by Simqke and RSPMatch. The ductility response indicates that the wavelet adjusting procedure gives a lower bias. On the other hand, it should be recalled that the RSPMatch records are the same records as the URR class to which the adjustment procedure was applied. Linearly scaled records, indifferently if moderately or significantly, seem to show no trends with respect to the URR class, although the large scattering of real records with respect to the target leads to large variability of the average estimated response from class to class of real records; see e.g., Fig. 6(c) and (d).

Fig. 7 shows the normalized ductility results for EPP systems. The stiffness degrading behavior of these SDOF systems tends to confirm the conclusions found for EPH systems. However, when interpreting the results for these two backbones it should be recalled that the URR class had a linear demand which was already generally above that of the artificial records. Moreover, hypothesis tests (to follow) do not confirm these differences to be statistically significant.

Fig. 8 shows the normalized kinematic ductility demand for ESD systems; in this case the trends are less clear. For R factors up to 4 it is possible to recognize about the same trends found for the EPH and EPP systems, see Fig. 8(a) and (b), with some underestimation of nonlinear demand that is systematically about 100%, for artificial and adjusted records with respect to real records classes. For higher R-values (6 and 10), see Fig. 8(c) and (d), it is not possible to recognize the same trends; all classes except Simqke records show similar ductility demands. This has an explanation related to modeling of the nonlinear systems; in fact, for R equal to 6 and 10, the ESD SDOF systems exceed the *ductility limit* and start cycling on the residual strength branch of the backbone. This behavior, which is systematic for all record classes, has a smoothing effect on the differences among the classes of accelerograms. However, it seems to be confirmed also for ESD systems that the SF5 and SF12 classes do not show any trend with respect to the URR class.

4.3. Equivalent number of cycles

N_e has the mentioned advantage of normalizing the cyclic response with respect to the peak demand, Eq. (5), allowing a comparison between the different classes of records in terms of cumulative demand only. Fig. 9 shows the values of this EDP for the EPH systems at different R-values. For all the R

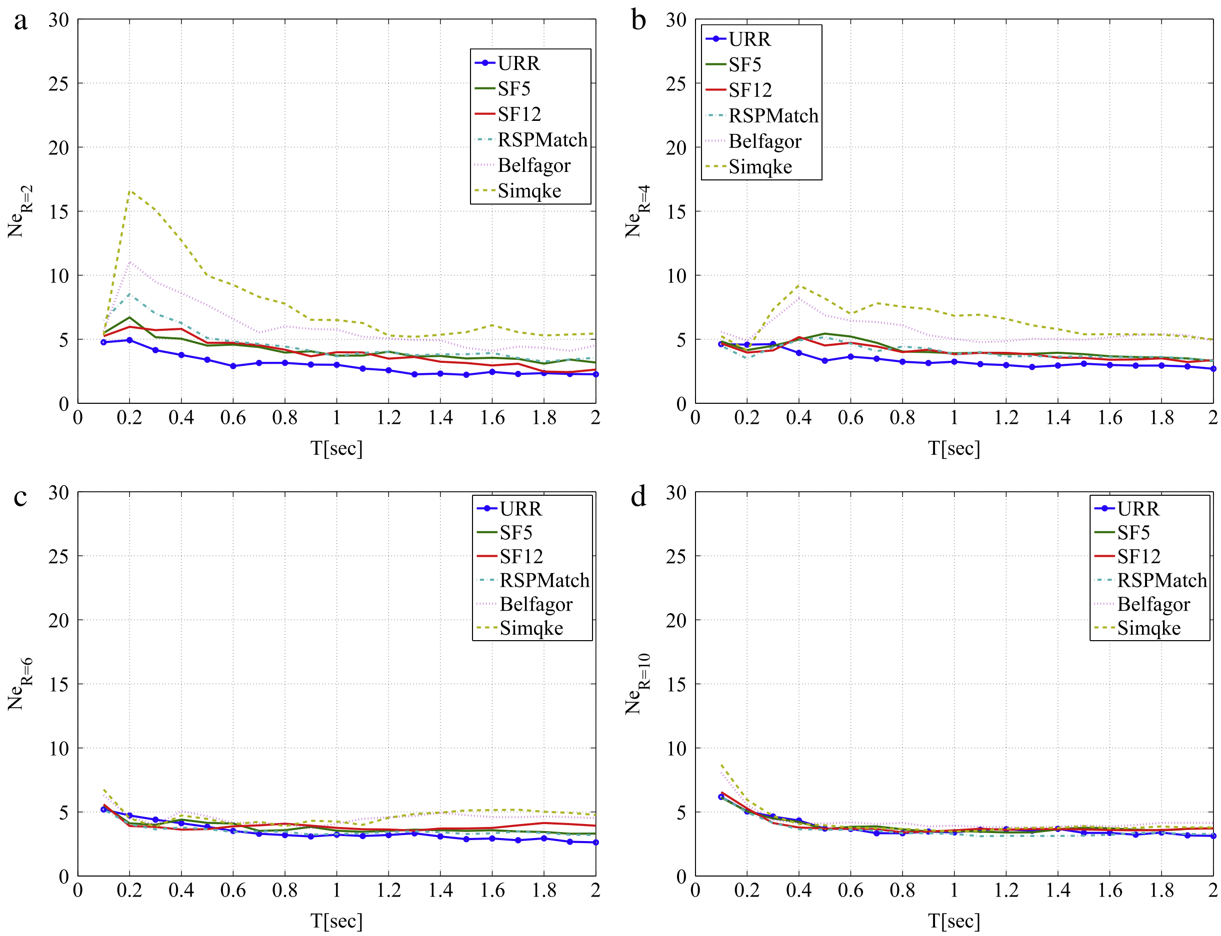

Fig. 11. Average values of the equivalent number of cycles for the ESD system computed as the mean value of 28 records.

investigated, a strong overestimation in terms of cyclic response may be observed for both classes of artificial records. Simqke records show the highest overestimation (e.g., twice that of the URR class at low periods). The Belfagor results show that a generation procedure based on non-stationary characteristics of the earthquake gives more acceptable results in terms of cyclic response. The cyclic EDP results seem to be independent of the strength reduction factor, at least for R-values ranging from 4 to 10. The latter is an expected result, in fact; N_e represents the total hysteretic energy normalized with respect to energy of the largest cycle.

The SF5 and SF12 records have, again, a non-systematic trend with respect to the URR class, confirming that the scaling procedure does not introduce any bias even if the scaling factor is large. The RSPMatch records give results very close to those of the URR class, indicating that the wavelet adjustment does not influence the cyclic response.

Fig. 10 shows the N_e results for the EPP systems. The same conclusions found for EPH systems hold. In this case the lower reduction factors (2, 4) are characterized by the largest N_e; this effect is strictly related to a decrease in the total hysteretic energy with the strength reduction factor.

Fig. 11 shows N_e for the ESD systems. Again, the same trends found for the EPH and EPP systems hold. The artificial records show cyclic response overestimation, while wavelet adjustment seems to introduce no bias with respect to the URR class. The moderately and significantly scaled real records also show no trends. Note that, for large strength reduction factors (6, 10), N_e tends to be similar for all classes. This is because ESD systems, at high nonlinearity level, easily reach the residual strength branch of the backbone.

4.4. Prediction of cyclic response

Cyclic response overestimation of artificial records was a predictable result; in fact, artificial records are characterized by higher values of the integral parameters, especially I_D. Fig. 12 shows, as an example, the I_D versus N_e plot of each record for EPH systems with R equal to 4, at two periods equal to 0.6 and 1.0 s, Fig. 12(a) and (b), respectively. Fig. 13 shows the I_D versus N_e plot for two EPP systems characterized by the same R at the same periods of Fig. 12. Similarly to the EPH systems, it is possible to note a fairly good correlation between the two parameters. Fig. 14 refers to ESD systems; in this case, the correlation is still good, but it becomes less recognizable for higher R-values due to fact that at these nonlinearity levels the *ductility limit* of the degrading system does not emphasize differences between the equivalent number of cycles response of each class (i.e., Fig. 11(c) and (d)).

As a conclusion, considering I_D evaluated in Section 2.5 for all record classes, and their compliance with the conditional hazard analysis, the latter can be suggested as an additional criterion in selection or generation procedures for accelerograms when the cyclic response represents a critical performance parameter for the structure to be analyzed.

5. Hypothesis tests

To finally draw conclusions from the results above, it may be helpful to try to quantitatively assess their significance. In

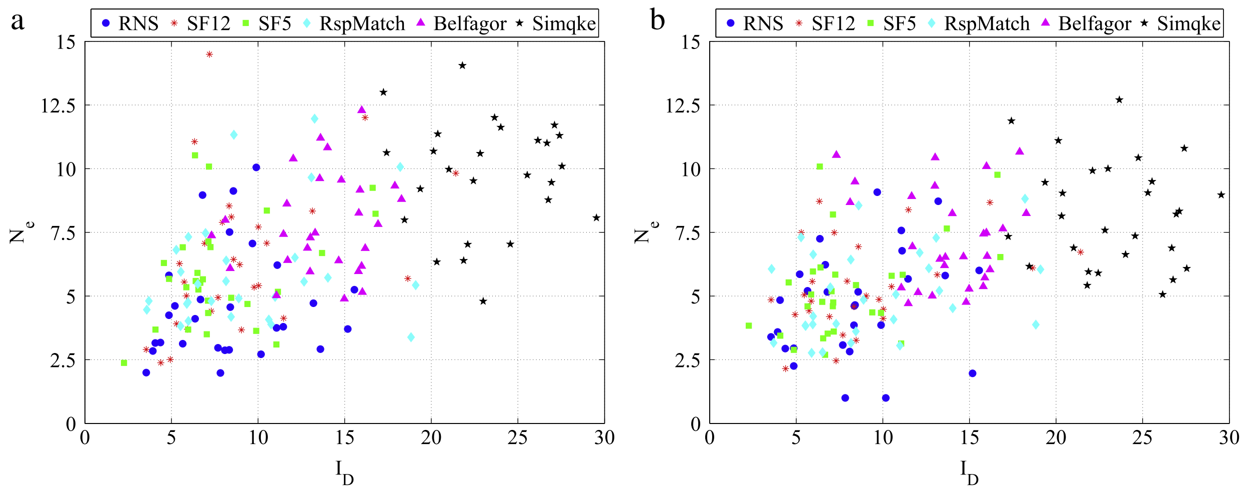

Fig. 12. N_e versus I_D for $R = 4$ and $T = 0.6$ s (a) and $T = 1.0$ s (b) evaluated for the EPH system for each record of each class.

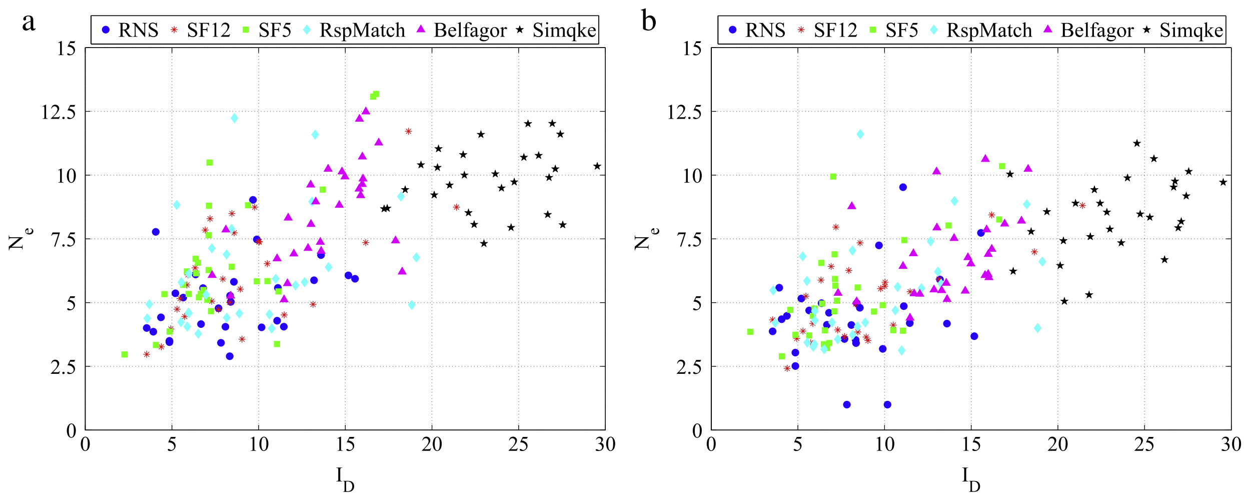

Fig. 13. N_e versus I_D for $R = 4$ and $T = 0.6$ s (a) and $T = 1.0$ s (b) evaluated for the EPP system for each record of each class.

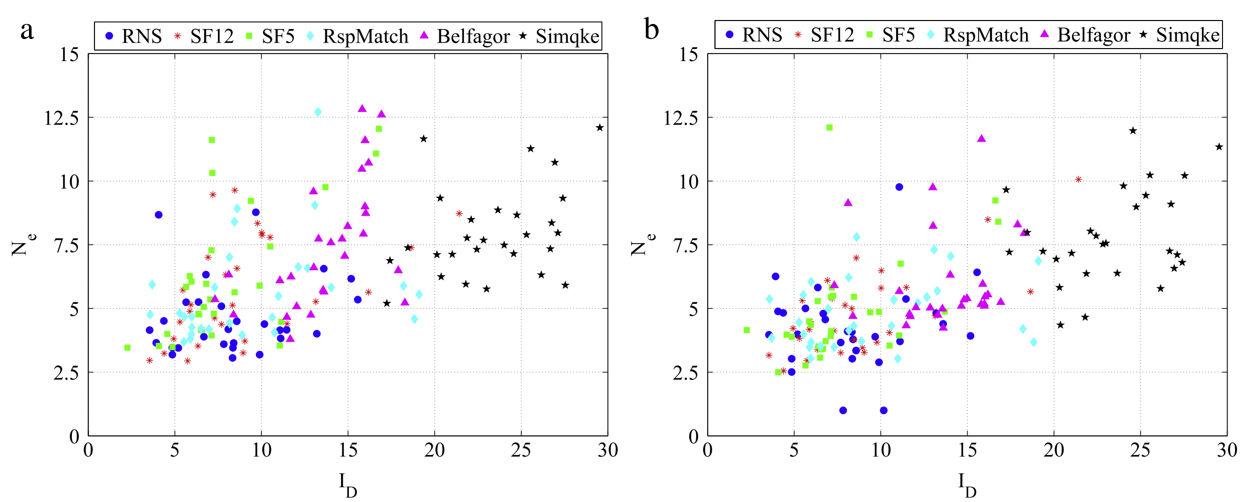

Fig. 14. N_e versus I_D for $R = 4$ and $T = 0.6$ s (a) and $T = 1.0$ s (b) evaluated for the ESD system for each record of each class.

particular, parametric hypothesis tests [29] were performed to assess to what significance the median values of the response, from a given class of records, may be considered equal to that from the URR class for each oscillation period in the considered range. Hypothesis tests were performed for both peak and cyclic EDPs. Regarding the peak response inelastic displacement, $Sd_{R=i}$

Table 2
Aspin–Welch test results for elastic displacements; *p*-values lower than 0.05 are reported in bold.

Period (s)		0.2	0.4	0.6	0.8	1	1.2	1.4	1.6	1.8	2
Compared		$R = 1$									
URR	SF12	0.882	0.328	0.178	0.308	0.382	0.379	0.467	0.676	0.647	0.699
URR	SF5	0.997	0.390	0.243	0.682	0.666	0.462	0.361	0.323	0.282	0.281
URR	RSPM	0.895	0.172	0.271	0.312	0.278	0.249	0.229	0.273	0.295	0.194
URR	Belf	0.878	0.183	0.230	0.362	0.308	0.258	0.215	0.281	0.323	0.229
URR	Simq	0.826	0.162	0.237	0.284	0.246	0.189	0.192	0.195	0.220	0.172

Table 3
Aspin–Welch test results for inelastic displacements of the EPH system; *p*-values lower than 0.05 are reported in bold.

Period (s)		0.2	0.4	0.6	0.8	1	1.2	1.4	1.6	1.8	2
Compared		$R = 2$									
URR	SF12	0.903	0.505	0.533	0.822	0.618	0.430	0.728	0.800	0.392	0.352
URR	SF5	0.777	0.528	0.564	0.932	0.690	0.652	0.360	0.276	0.248	0.220
URR	RSPM	0.914	0.521	0.534	0.737	0.381	0.362	0.250	0.270	0.183	0.119
URR	Belf	0.990	0.603	0.673	0.540	0.841	0.918	0.997	0.793	0.566	0.389
URR	Simq	0.623	0.089	0.227	0.638	0.643	0.309	0.320	0.211	0.230	0.057
Compared		$R = 4$									
URR	SF12	0.389	0.498	0.920	0.578	0.421	0.389	0.398	0.355	0.269	0.292
URR	SF5	0.279	0.830	0.512	0.966	0.530	0.362	0.255	0.162	0.134	0.166
URR	RSPM	0.813	0.723	0.495	0.946	0.590	0.599	0.387	0.218	0.140	0.124
URR	Belf	0.761	0.884	0.420	0.466	0.617	0.782	0.980	0.956	0.995	0.991
URR	Simq	0.803	0.530	0.826	0.932	0.715	0.496	0.170	0.165	0.113	0.069
Compared		$R = 6$									
URR	SF12	0.358	0.736	0.768	0.435	0.612	0.459	0.354	0.423	0.426	0.516
URR	SF5	0.366	0.956	0.853	0.469	0.661	0.446	0.288	0.177	0.158	0.228
URR	RSPM	0.891	0.927	0.960	0.969	0.730	0.426	0.244	0.179	0.190	0.319
URR	Belf	0.830	0.793	0.867	0.378	0.559	0.830	0.908	0.945	0.998	0.849
URR	Simq	0.745	0.846	0.797	0.909	0.787	0.487	0.323	0.206	0.137	0.318
Compared		$R = 10$									
URR	SF12	0.460	0.562	0.517	0.587	0.656	0.607	0.479	0.600	0.679	0.880
URR	SF5	0.545	0.825	0.578	0.477	0.534	0.436	0.260	0.295	0.365	0.325
URR	RSPM	0.764	0.923	0.977	0.787	0.520	0.478	0.266	0.316	0.461	0.554
URR	Belf	0.290	0.155	0.142	0.148	0.503	0.821	0.690	0.792	0.894	0.781
URR	Simq	0.788	0.657	0.601	0.581	0.872	0.754	0.410	0.417	0.399	0.327

Table 4
Aspin–Welch test results for inelastic displacements of the EPP system; *p*-values lower than 0.05 are reported in bold.

Period (s)		0.2	0.4	0.6	0.8	1	1.2	1.4	1.6	1.8	2
Compared		$R = 2$									
URR	SF12	0.620	0.690	0.826	0.630	0.610	0.585	0.730	0.669	0.475	0.528
URR	SF5	0.878	0.710	0.824	0.928	0.749	0.712	0.350	0.289	0.270	0.230
URR	RSPM	0.541	0.770	0.835	0.822	0.483	0.590	0.429	0.365	0.164	0.131
URR	Belf	0.543	0.815	0.645	0.475	0.638	0.890	0.973	0.757	0.664	0.644
URR	Simq	0.976	0.633	0.789	0.625	0.896	0.787	0.608	0.738	0.457	0.388
Compared		$R = 4$									
URR	SF12	0.366	0.394	0.613	0.516	0.507	0.520	0.321	0.329	0.395	0.445
URR	SF5	0.490	0.680	0.805	0.741	0.494	0.407	0.260	0.204	0.193	0.212
URR	RSPM	0.591	0.626	0.699	0.816	0.677	0.433	0.238	0.185	0.152	0.193
URR	Belf	0.424	0.768	0.314	0.247	0.718	0.773	0.741	0.730	0.543	0.605
URR	Simq	0.350	0.911	0.783	0.365	0.735	0.895	0.612	0.324	0.360	0.404
Compared		$R = 6$									
URR	SF12	0.273	0.328	0.422	0.428	0.523	0.444	0.385	0.499	0.713	0.849
URR	SF5	0.574	0.831	0.633	0.396	0.436	0.362	0.237	0.202	0.256	0.298
URR	RSPM	0.669	0.919	0.642	0.683	0.485	0.287	0.207	0.178	0.222	0.239
URR	Belf	0.878	0.559	0.432	0.592	0.804	0.649	0.774	0.791	0.713	0.671
URR	Simq	0.465	0.966	0.693	0.667	0.846	0.766	0.499	0.453	0.528	0.487
Compared		$R = 10$									
URR	SF12	0.195	0.313	0.346	0.488	0.504	0.487	0.616	0.868	0.977	0.975
URR	SF5	0.494	0.508	0.314	0.372	0.377	0.253	0.254	0.402	0.465	0.468
URR	RSPM	0.489	0.508	0.494	0.420	0.291	0.218	0.214	0.364	0.487	0.404
URR	Belf	0.487	0.415	0.720	0.533	0.637	0.795	0.957	0.944	0.948	0.941
URR	Simq	0.503	0.967	0.898	0.951	0.908	0.589	0.498	0.549	0.542	0.452

($i = 1, 2, 4, 6, 10$) was chosen as the variable to test, and it was considered to have a lognormal distribution. What is found for the inelastic displacement is valid also for D_{kin}, see Eq. (4), considering the *constant strength approach* adopted. Regarding cyclic response,

Table 5
Aspin–Welch test results for inelastic displacements of the ESD system; *p*-values lower than 0.05 are reported in bold.

Period (s)		0.2	0.4	0.6	0.8	1.0	1.2	1.4	1.6	1.8	2.0
Compared		$R = 2$									
URR	SF12	0.491	0.981	0.914	0.654	0.761	0.747	0.864	0.709	0.545	0.552
URR	SF5	0.163	0.976	0.692	0.909	0.795	0.839	0.326	0.292	0.278	0.228
URR	RSPM	0.072	0.849	0.874	0.672	0.725	0.868	0.571	0.426	0.210	0.156
URR	Belf	0.080	0.882	0.434	0.416	0.438	0.648	0.772	0.879	0.845	0.738
URR	Simq	0.208	0.955	0.629	0.559	0.670	0.975	0.744	0.853	0.579	0.432
Compared		$R = 4$									
URR	SF12	**0.013**	0.796	0.883	0.460	0.457	0.475	0.454	0.420	0.496	0.600
URR	SF5	**0.046**	0.881	0.835	0.483	0.365	0.306	0.210	0.177	0.209	0.242
URR	RSPM	**0.010**	0.787	0.467	0.553	0.725	0.462	0.233	0.214	0.226	0.200
URR	Belf	**0.003**	0.212	0.364	0.443	0.845	0.743	0.786	0.714	0.481	0.513
URR	Simq	**0.000**	0.729	0.818	0.460	0.660	0.850	0.585	0.429	0.426	0.469
Compared		$R = 6$									
URR	SF12	**0.001**	**0.011**	0.112	0.474	0.520	0.444	0.590	0.909	0.529	0.661
URR	SF5	**0.004**	0.103	0.282	0.275	0.311	0.224	0.203	0.274	0.488	0.510
URR	RSPM	**0.027**	**0.036**	0.140	0.319	0.207	0.260	0.231	0.269	0.490	0.469
URR	Belf	**0.001**	**0.011**	**0.030**	0.210	0.556	0.750	0.502	0.535	0.271	0.270
URR	Simq	**0.000**	**0.000**	**0.000**	**0.002**	**0.017**	0.055	0.168	0.314	0.615	0.598
Compared		$R = 10$									
URR	SF12	**0.047**	**0.007**	0.114	0.114	0.253	0.275	0.366	0.564	0.650	0.930
URR	SF5	**0.012**	0.062	0.207	0.281	0.187	0.147	0.365	0.524	0.461	0.576
URR	RSPM	0.135	**0.015**	0.335	0.188	0.158	**0.046**	0.100	0.280	0.344	0.374
URR	Belf	**0.011**	**0.002**	0.079	0.278	0.337	0.258	0.621	0.948	0.612	0.439
URR	Simq	**0.005**	**0.000**	**0.002**	**0.004**	**0.002**	**0.003**	**0.008**	**0.027**	**0.038**	**0.042**

Table 6
Aspin–Welch test results for equivalent number of cycles of the EPH system; *p*-values lower than 0.05 are reported in bold.

Period (s)		0.2	0.4	0.6	0.8	1	1.2	1.4	1.6	1.8	2
Compared		$R = 2$									
URR	SF12	0.812	**0.028**	**0.037**	**0.012**	0.101	0.224	**0.044**	**0.046**	0.587	0.658
URR	SF5	0.992	0.166	0.114	0.439	0.365	0.128	**0.043**	0.170	0.243	0.142
URR	RSPM	0.427	**0.003**	**0.033**	**0.018**	0.389	0.161	**0.036**	**0.026**	0.051	**0.015**
URR	Belf	**0.040**	**0.000**	**0.001**	**0.024**	**0.001**	**0.002**	**0.000**	**0.000**	**0.001**	**0.001**
URR	Simq	**0.000**	**0.000**	**0.000**	**0.000**	**0.000**	**0.002**	**0.000**	**0.000**	**0.000**	**0.001**
Compared		$R = 4$									
URR	SF12	0.597	0.071	**0.010**	**0.021**	0.116	0.074	0.177	0.307	0.593	0.402
URR	SF5	0.339	0.303	**0.024**	**0.036**	0.167	0.199	**0.045**	0.131	0.157	0.146
URR	RSPM	0.526	0.078	**0.010**	0.173	0.298	**0.043**	**0.020**	**0.028**	**0.044**	**0.047**
URR	Belf	**0.004**	**0.000**	**0.000**	**0.000**	**0.000**	**0.000**	**0.000**	**0.000**	**0.000**	**0.000**
URR	Simq	**0.000**	**0.000**	**0.000**	**0.000**	**0.000**	**0.000**	**0.000**	**0.000**	**0.000**	**0.000**
Compared		$R = 6$									
URR	SF12	0.781	**0.033**	0.019	**0.044**	**0.019**	0.139	0.158	0.193	0.459	0.195
URR	SF5	0.641	0.212	0.060	0.207	**0.023**	0.091	**0.045**	0.069	0.250	0.129
URR	RSPM	0.294	0.133	0.092	0.156	0.085	0.087	**0.046**	0.056	0.105	**0.020**
URR	Belf	**0.000**	**0.000**	**0.000**	**0.000**	**0.000**	**0.000**	**0.000**	**0.000**	**0.001**	**0.000**
URR	Simq	**0.000**	**0.000**	**0.000**	**0.000**	**0.000**	**0.000**	**0.000**	**0.000**	**0.000**	**0.000**
Compared		$R = 10$									
URR	SF12	0.408	**0.049**	0.059	**0.022**	**0.026**	0.070	0.180	0.148	0.202	0.081
URR	SF5	0.891	0.252	0.231	0.140	0.072	0.083	0.221	0.153	0.162	0.192
URR	RSPM	0.314	0.129	0.092	0.071	0.098	**0.033**	0.111	0.061	**0.029**	**0.013**
URR	Belf	**0.000**	**0.000**	**0.000**	**0.000**	**0.000**	**0.000**	**0.001**	**0.001**	**0.000**	**0.000**
URR	Simq	**0.000**	**0.000**	**0.000**	**0.000**	**0.000**	**0.000**	**0.000**	**0.000**	**0.000**	**0.000**

$N_e + 1$ was chosen as the variable to test, again, with a lognormal distribution.[4]

The null hypothesis to check was whether the median EDPs for any class of records were equal (null hypothesis) or not (alternate hypothesis) to that from the URR class. To this aim, a two-tail Aspin–Welch test [31] was preferred with respect to the standard Student *t*-test, as the former does not require the assumption of equal, yet still unknown, variances of populations originating the samples, which would be an unreasonable assumption given the natures of the compared record classes.

The test statistic employed is reported in Eq. (6), in which z_x and z_y are the sample means, s_x and s_y are the sample standard deviations and n and m are the samples sizes (in this case always equal to 28). The test statistic, under the null hypothesis, has an approximate Student-*t* distribution with the number of degrees of freedom given by Satterthwaite's approximation [32].

$$t = \frac{z_x - z_y}{\sqrt{\frac{s_x^2}{n} + \frac{s_y^2}{m}}}. \qquad (6)$$

[4] The distribution assumptions were checked with the Lilliefors test [30], and could not be rejected at the 95% significance level.

Table 7
Aspin–Welch test results for equivalent number of cycles of the EPP system; p-values lower than 0.05 are reported in bold.

Period (s)		0.2	0.4	0.6	0.8	1	1.2	1.4	1.6	1.8	2
Compared		$R = 2$									
URR	SF12	0.571	**0.004**	**0.011**	**0.032**	0.092	0.051	0.054	0.180	0.394	0.322
URR	SF5	0.221	**0.025**	**0.009**	0.121	0.077	**0.013**	**0.010**	0.107	0.193	0.093
URR	RSPM	**0.047**	**0.002**	**0.003**	**0.020**	0.069	**0.007**	**0.001**	**0.002**	**0.008**	**0.001**
URR	Belf	**0.000**	**0.000**	**0.000**	**0.000**	**0.000**	**0.000**	**0.000**	**0.000**	**0.000**	**0.000**
URR	Simq	**0.000**	**0.000**	**0.000**	**0.000**	**0.000**	**0.000**	**0.000**	**0.000**	**0.000**	**0.000**
Compared		$R = 4$									
URR	SF12	0.396	0.060	**0.047**	**0.028**	0.065	0.051	0.250	0.292	0.500	0.196
URR	SF5	0.787	0.195	**0.020**	**0.030**	**0.061**	0.068	**0.018**	0.084	0.160	0.129
URR	RSPM	0.463	0.284	**0.038**	**0.021**	0.059	**0.034**	**0.023**	**0.027**	**0.048**	**0.020**
URR	Belf	**0.000**	**0.000**	**0.000**	**0.000**	**0.000**	**0.000**	**0.000**	**0.000**	**0.000**	**0.000**
URR	Simq	**0.000**	**0.000**	**0.000**	**0.000**	**0.000**	**0.000**	**0.000**	**0.000**	**0.000**	**0.000**
Compared		$R = 6$									
URR	SF12	0.345	0.149	0.061	0.126	0.200	0.236	0.254	0.169	0.116	**0.031**
URR	SF5	0.413	0.092	0.070	0.194	0.105	0.091	0.109	0.142	0.278	0.114
URR	RSPM	0.482	0.137	0.221	0.082	0.101	0.127	0.114	0.125	0.201	0.075
URR	Belf	**0.000**	**0.000**	**0.000**	**0.000**	**0.000**	**0.000**	**0.000**	**0.000**	**0.000**	**0.000**
URR	Simq	**0.000**	**0.000**	**0.000**	**0.000**	**0.000**	**0.000**	**0.000**	**0.000**	**0.000**	**0.000**
Compared		$R = 10$									
URR	SF12	0.463	0.131	0.230	0.144	0.282	0.359	0.347	0.059	0.047	0.027
URR	SF5	0.320	0.165	0.369	0.231	0.259	0.537	0.744	0.240	0.213	0.125
URR	RSPM	0.731	0.514	0.176	0.143	0.382	0.494	0.770	0.210	0.124	0.120
URR	Belf	**0.000**	**0.000**	**0.000**	**0.000**	**0.000**	**0.000**	**0.004**	**0.002**	**0.006**	**0.006**
URR	Simq	**0.000**	**0.000**	**0.000**	**0.000**	**0.000**	**0.000**	**0.000**	**0.000**	**0.000**	**0.000**

Table 8
Aspin–Welch test results for equivalent number of cycles of the ESD system; p-values lower than 0.05 are reported in bold.

Period (s)		0.2	0.4	0.6	0.8	1.0	1.2	1.4	1.6	1.8	2.0
Compared		$R = 2$									
URR	SF12	0.116	**0.002**	**0.009**	**0.034**	0.076	**0.046**	0.051	0.189	0.347	0.337
URR	SF5	**0.022**	**0.013**	**0.007**	0.105	0.058	**0.007**	**0.015**	0.125	0.219	0.105
URR	RSPM	**0.002**	**0.001**	**0.001**	**0.015**	**0.047**	**0.004**	**0.001**	**0.002**	**0.006**	**0.002**
URR	Belf	**0.000**	**0.000**	**0.000**	**0.000**	**0.000**	**0.000**	**0.000**	**0.000**	**0.000**	**0.000**
URR	Simq	**0.000**	**0.000**	**0.000**	**0.000**	**0.000**	**0.000**	**0.000**	**0.000**	**0.000**	**0.000**
Compared		$R = 4$									
URR	SF12	0.094	**0.028**	**0.035**	0.084	0.131	0.063	0.135	0.227	0.350	0.108
URR	SF5	0.263	**0.036**	**0.007**	0.084	0.141	0.124	**0.033**	0.154	0.195	0.140
URR	RSPM	**0.002**	0.108	**0.018**	**0.007**	0.076	0.056	**0.037**	**0.043**	**0.048**	**0.041**
URR	Belf	0.464	**0.000**	**0.000**	**0.000**	**0.000**	**0.000**	**0.000**	**0.000**	**0.000**	**0.000**
URR	Simq	0.312	**0.000**	**0.000**	**0.000**	**0.000**	**0.000**	**0.000**	**0.000**	**0.000**	**0.000**
Compared		$R = 6$									
URR	SF12	**0.020**	0.167	0.408	0.065	0.168	0.218	0.095	**0.028**	**0.003**	**0.003**
URR	SF5	0.105	0.770	0.345	0.422	0.418	0.389	0.209	0.127	0.151	0.053
URR	RSPM	0.067	0.267	0.592	0.417	0.905	0.382	0.235	0.183	0.182	0.065
URR	Belf	0.989	0.181	0.063	**0.009**	**0.007**	**0.000**	**0.000**	**0.000**	**0.000**	**0.000**
URR	Simq	0.829	0.368	0.103	**0.036**	**0.015**	**0.004**	**0.001**	**0.000**	**0.000**	**0.000**
Compared		$R = 10$									
URR	SF12	0.417	0.079	0.707	0.530	0.390	0.675	0.630	0.272	0.325	0.070
URR	SF5	0.947	0.652	0.735	0.439	0.769	0.782	0.896	0.306	0.394	0.133
URR	RSPM	0.964	**0.023**	0.829	0.736	0.963	0.394	0.345	0.910	0.736	0.362
URR	Belf	0.085	0.662	**0.033**	**0.007**	0.073	0.330	0.329	0.062	**0.024**	**0.005**
URR	Simq	**0.003**	0.508	0.337	0.088	0.382	0.497	0.457	0.153	0.118	**0.042**

Because the URR class was assumed as a benchmark, a preliminary test was performed to check if it was possible to reject the null hypothesis in terms of elastic displacement first. Table 2 presents the p-values divided per period; bold values are the rejection cases assuming a 95% significance level; i.e., choosing I-type risk (α) equal to 0.05. The period values reported in the hypothesis test tables are steps of 0.2 s for the sake of brevity.

Tables 3–5 show the test results for different R-values (2, 4, 6, 10) and for the EPH, EPP and ESD SDOF models, respectively. The results presented in Table 3 show that there are no rejections with respect to the URR class at any reduction factor. Results in term of displacements are qualitatively similar to EPH with no rejections (Table 4). From Table 5, it is seen that there are a number of rejections in comparing real and artificial accelerograms. It is worth noting that, in this case, the results relative to high R-values (6, 10) are affected by the fact that the ductility demand exceeds the *ductility limit* and rejections associated to Simqke records indicate displacements significantly higher than those of real records; see Fig. 8(c) and (d).

Tables 6–8 show test results for different R-values on equivalent numbers of cycles for the EPH, EPP and ESD systems, respectively. As was expected, considering the results in Section 4.3, there are a large number of rejections for this EDP for all kinds of SDOF models,

Table A.1
Information for the URR records according to the European Strong Motion Database.

Set	Waveform no.	Earthquake no.	Earthquake name	Date	M_w	Fault mechanism	R_e (km)
I	365*y*	175	Lazio Abruzzo	07/05/1984	5.9	Normal	5
	4674*x*	1635	South Iceland	17/06/2000	6.5	Strike slip	5
	4675*y*	1635	South Iceland	17/06/2000	6.5	Strike slip	13
	4675*x*	1635	South Iceland	17/06/2000	6.5	Strike slip	13
	6326*y*	2142	South Iceland (aftershock)	21/06/2000	6.4	Strike slip	14
	6332*x*	2142	South Iceland (aftershock)	21/06/2000	6.4	Strike slip	6
	6335*x*	2142	South Iceland (aftershock)	21/06/2000	6.4	Strike slip	15
II	182*y*	87	Tabas	16/09/1978	7.3	Oblique	12
	242*x*	115	Valnerina	19/09/1979	5.8	Normal	5
	242*y*	115	Valnerina	19/09/1979	5.8	Normal	5
	1231*x*	472	Izmit	17/08/1999	7.6	Strike slip	9
	1231*y*	472	Izmit	17/08/1999	7.6	Strike slip	9
	3802*x*	1226	SE of Tirana	09/01/1988	5.9	Thrust	7
	7142*y*	2309	Bingol	01/05/2003	6.3	Strike slip	14
III	234*x*	108	Montenegro (aftershock)	24/05/1979	6.2	Thrust	30
	287*x*	146	Campano Lucano	23/11/1980	6.9	Normal	23
	287*y*	146	Campano Lucano	23/11/1980	6.9	Normal	23
	290*x*	146	Campano Lucano	23/11/1980	6.9	Normal	32
	665*x*	286	Umbria Marche	26/09/1997	6	Normal	21
	6500*x*	497	Duzce 1	12/11/1999	7.2	Oblique	23
	7156*x*	2313	Firuzabad	20/06/1994	5.9	Strike slip	21
IV	55*x*	34	Friuli	06/05/1976	6.5	Thrust	23
	198*x*	93	Montenegro	15/04/1979	6.9	Thrust	21
	198*y*	93	Montenegro	15/04/1979	6.9	Thrust	21
	4678*x*	1635	South Iceland	17/06/2000	6.5	Strike slip	32
	6342*x*	2142	South Iceland (aftershock)	21/06/2000	6.4	Strike slip	20
	6342*y*	2142	South Iceland (aftershock)	21/06/2000	6.4	Strike slip	20
	7187*x*	2322	Avej	22/06/2002	6.5	Thrust	28

Table A.2
Information and SF factors for the SF5 records according to the European Strong Motion Database.

Set	Waveform no.	Earthquake no.	Earthquake name	Date	M_w	Mechanism	R_e (km)	SF
I	234*y*	108	Montenegro (aftershock)	24/05/1979	6.2	Thrust	30	2.499
	292*x*	146	Campano Lucano	23/11/1980	6.9	Normal	25	3.206
	292*y*	146	Campano Lucano	23/11/1980	6.9	Normal	25	3.207
	368*x*	175	Lazio Abruzzo	07/05/1984	5.9	Normal	22	3.000
	410*x*	189	Golbasi	05/05/1986	6	Oblique	29	4.918
	5272*x*	1338	Mt. Vatnafjoll	25/05/1987	6	Oblique	24	5.848
	6262*y*	1635	South Iceland	17/06/2000	6.5	Strike slip	31	2.848
II	182*y*	87	Tabas	16/09/1978	7.3	Oblique	12	0.499
	182*x*	87	Tabas	16/09/1978	7.3	Oblique	12	0.568
	471*y*	227	Vrancea	30/05/1990	6.9	Thrust	6	8.037
	1243*x*	473	Izmit (aftershock)	13/09/1999	5.8	Oblique	15	2.640
	4674	1635	South Iceland	17/06/2000	6.5	Strike slip	5	0.604
	4675*x*	1635	South Iceland	17/06/2000	6.5	Strike slip	13	1.459
	7142*y*	2309	Bingol	01/05/2003	6.3	Strike slip	14	0.646
III	55*x*	34	Friuli	06/05/1976	6.5	Thrust	23	0.539
	55*y*	34	Friuli	06/05/1976	6.5	Thrust	23	0.608
	6327*y*	2142	South Iceland (aftershock)	21/06/2000	6.4	Strike slip	24	3.241
	6331*y*	2142	South Iceland (aftershock)	21/06/2000	6.4	Strike slip	22	4.881
	6331*x*	2142	South Iceland (aftershock)	21/06/2000	6.4	Strike slip	22	3.673
	6333*x*	2142	South Iceland (aftershock)	21/06/2000	6.4	Strike slip	28	9.450
	7187*x*	2322	Avej	22/06/2002	6.5	Thrust	28	0.431
IV	473*y*	228	Vrancea	31/05/1990	6.3	Thrust	7	21.822
	3802*x*	1226	SE of Tirana	09/01/1988	5.9	Thrust	7	1.693
	6326*y*	2142	South Iceland (aftershock)	21/06/2000	6.4	Strike slip	14	1.649
	6332*x*	2142	South Iceland (aftershock)	21/06/2000	6.4	Strike slip	6	0.363
	6335*y*	2142	South Iceland (aftershock)	21/06/2000	6.4	Strike slip	15	1.664
	6335*x*	2142	South Iceland (aftershock)	21/06/2000	6.4	Strike slip	15	1.510
	6349*y*	2142	South Iceland (aftershock)	21/06/2000	6.4	Strike slip	5	0.229

especially for Belfagor and Simqke accelerograms. The RSPMatch records do not lead to a significant number of rejections.

For ESD models (Table 8), rejections at all periods always indicate an overestimation of artificial records. The number of rejections tends to reduce at high nonlinearity levels. In fact, in the previous section it was observed that, when the ductility demand exceeds the *ductility limit*, the equivalent number of cycles tends to be similar for all six classes. The scaled real records present only a few rejections with respect to the URR records.

6. Conclusions

In this work, different ways to achieve spectrum matching record sets were compared in terms of post-elastic seismic peak and cyclic responses. This was pursued by considering SDOF systems with three different force–displacement backbones and hysteretic rules at different nonlinearity levels. The ductility and equivalent number of cycles response of 240 systems were analyzed with respect to six classes of records: real unscaled, real

Table A.3
Information and SF factors for the SF12 records according to the European Strong Motion Database.

Set	Waveform no.	Earthquake no.	Earthquake name	Date	M_w	Mechanism	R_e (km)	SF
I	169*x*	80	Calabria	11/03/1978	5.2	Normal	10	2.539
	382*y*	176	Lazio Abruzzo (aftershock)	11/05/1984	5.5	Normal	16	12.811
	383*x*	176	Lazio Abruzzo (aftershock)	11/05/1984	5.5	Normal	14	9.502
	5078*x*	1464	Mt. Hengill Area	04/06/1998	5.4	Strike slip	18	14.219
	5085*x*	1464	Mt. Hengill Area	04/06/1998	5.4	Strike slip	15	15.714
	5086*x*	1464	Mt. Hengill Area	04/06/1998	5.4	Strike slip	15	8.396
	5090*x*	1464	Mt. Hengill Area	04/06/1998	5.4	Strike slip	18	6.128
II	95*y*	52	Friuli (aftershock)	17/06/1976	5.2	Oblique	26	21.301
	95*x*	52	Friuli (aftershock)	17/06/1976	5.2	Oblique	26	19.028
	642*y*	292	Umbria Marche (aftershock)	14/10/1997	5.6	Normal	23	3.049
	1891*y*	651	Kranidia	25/10/1984	5.5	?	23	7.382
	1893*y*	652	Near SW coast of Peloponnese	10/12/1987	5.2	?	30	11.385
	5089*y*	1464	Mt. Hengill Area	04/06/1998	5.4	Strike slip	23	11.917
	5895*y*	1932	Arnissa	09/07/1984	5.2	Normal	30	17.543
III	847*x*	363	Umbria Marche (aftershock)	26/03/1998	5.4	Oblique	41	8.620
	1884*y*	229	Filippias	16/06/1990	5.5	Thrust	43	16.711
	1899*x*	657	Gulf of Kiparissiakos	07/09/1985	5.4	Oblique	37	9.182
	1994*x*	645	Skydra-Edessa	18/02/1986	5.3	?	31	18.973
	4560*y*	1387	Bovec	12/04/1998	5.6	Strike slip	38	19.425
	5087*x*	1464	Mt. Hengill Area	04/06/1998	5.4	Strike slip	32	28.143
	7089*x*	2290	Pasinler	10/07/2001	5.4	Strike slip	32	9.833
IV[a]	410*x*	189	Golbasi	05/05/1986	6	Oblique	29	5.918
	471*y*	227	Vrancea	30/05/1990	6.9	Thrust	6	8.737
	473*y*	228	Vrancea	31/05/1990	6.3	Thrust	7	19.322
	1243*x*	473	Izmit (aftershock)	13/09/1999	5.8	Oblique	15	3.237
	5272*x*	1338	Mt. Vatnafjoll	25/05/1987	6	Oblique	24	10.848
	6761*y*	2222	Vrancea	30/08/1986	7.2	Thrust	49	1.439
	6761*x*	2222	Vrancea	30/08/1986	7.2	Thrust	49	1.100

[a] "Manually" selected and scaled.

with moderate linear scaling factor, real with significant linear scaling factor, real adjusted with wavelets, and two different types of artificial records.

The *life–safety* design elastic spectrum, for a case-study site in southern Italy, was considered; all the classes of records match it on average or by means of individual records.

Results indicate that the linearly scaled records do not show any systematic trend with respect to the unscaled record results independently of the backbone and response parameters, suggesting that scaling is a legitimate technique, as many studies point out, if the spectral shape is controlled.

The RSPMatch2005 wavelet-adjustment procedure shows small, if any, bias in terms of peak and cyclic responses. Conversely, both classes of artificial records, but especially non-stationary accelerograms, in some cases seem to underestimate the peak demand (ductility). The artificial records, especially those stationary, gave strong cyclic response overestimation (at least until the ductility demand let the hysteresis reach the residual strength of the backbone, although this is more a modeling issue).

Hypothesis tests were carried out with the aim of assessing quantitatively how significant these results are. Tests have shown a statistical significance of the bias of artificial records only in terms of cyclic response. Regarding the peak response, the test results suggest that underestimation of artificial records with respect to unscaled real records does not have statistical significance. In fact, it is significant only in the case of the degrading systems (ESD) at high nonlinearity levels, when modeling hypotheses have a strong influence.

It worth noting that, as is well known, the cyclic response overestimation could have been predicted by some integral parameters of ground motion, which, if an appropriate hazard analysis tool is available, could be used as an additional criterion for record selection, especially in those cases when cyclic behavior has an important role in determining the seismic performances.

Appendix

In this appendix, data regarding the real records selected are reported. Table A.1 collects, for the URR class, the record number and event number according to the European Strong Motion Database. Tables A.2 and A.3 collect the same information for the SF5 and SF12 classes, respectively (in these two tables the scaling factor applied to each single record is also reported). In the tables, *x* and *y* represent the two horizontal components of the record.

References

[1] Iervolino I, Maddaloni G, Cosenza E. Eurocode 8 compliant real record sets for seismic analysis of structures. J Earthq Eng 2008;12(1):54–90.
[2] Comité Européen de Normalisation. Eurocode8. Design of Structures for earthquake resistance–part1: general rules, seismic actions and rules for buildings. EN 1998-1, CEN. Brussels. 2003.
[3] Bommer JJ, Acevedo AB. The use of real earthquake accelerograms as input to dynamic analysis. J Earthq Eng 2004;8(I):43–91 [Special issue].
[4] CS LL PP; DM 14 Gennaio 2008 Norme tecniche per le costruzioni. Gazzetta Ufficiale della Repubblica Italiana, 29. 4/2/2008 [in Italian].
[5] Convertito V, Iervolino I, Herrero A. The importance of mapping the design earthquakes: insights for southern Italy. Bull Seismol Soc Am 2009;99(5): 2979–91.
[6] Iervolino I, Maddaloni G, Cosenza E. A note on selection of time-histories for seismic analysis of bridges in Eurocode 8. J Earthq Eng 2009;13(8):1125–52.
[7] Hancock J, Watson-Lamprey J, Abrahamson NA, Bommer JJ, Markatis A, McCoy E, Mendis E. An improved method of matching response spectra of recorded earthquake ground motion using wavelets. J Earthq Eng 2006;10(I): 67–89 [Special issue].
[8] Iervolino I, Cornell CA. Record selection for nonlinear seismic analysis of structures. Earthq Spect 2005;21(3):685–713.
[9] Schwab P, Lestuzzi P. Assessment of the seismic nonlinear behaviour of ductile wall structures due to synthetic earthquakes. Bull Earthq Eng 2007;5:67–84.
[10] Iervolino I, Manfredi G, Cosenza E. Ground motion duration effects on nonlinear seismic response. Earthq Eng Struct Dyn 2006;30:485–99.
[11] Manfredi G. Evaluation of seismic energy demand. Earthq Eng Struct Dyn 2001; 35:21–38.
[12] Esposito M. Accelerogrammi spettrocompatibili per la progettazione delle strutture: valutazione comparativa della risposta sismica. Graduation thesis: Dipartimento di Ingegneria Strutturale, Università degli Studi di Napoli Federico II. Advisors: Cosenza E, Iervolino I, De Luca F. 2009. Available at http://wpage.unina.it/iuniervo/ [in Italian].
[13] Iervolino I, Galasso C, Cosenza E. REXEL: computer aided record selection for code-based seismic structural analysis. Bull Earthq Eng 2009;8:339–62.

[14] Baker JW, Cornell CA. Spectral shape, epsilon and record selection. Earthq Eng Struct Dyn 2006;35(9):1077–95.
[15] Hancock J, Bommer JJ, Stafford PJ. Number of scaled and matched accelerograms required for inelastic dynamic analyses. Earthq Eng Struct Dyn 2008; 37(14):1585–607.
[16] PEER ground motion selection and modification working group. Haselton CB, editor. Evaluation of Ground Motion selection methods: prediction median interstory drift response of buildings. PEER report 2009/01. 2009. Available at http://peer.berkeley.edu/publications/peer_reports/reports_2009.
[17] Abrahamson NA. Non-stationary spectral matching. Seismol Res Lett 1992; 63(1):30.
[18] Grant DN, Greening PD, Taylor ML, Ghosh B. Seed record selection for spectral matching with RSPMatch2005. In: Proceedings of 14th world conference on earthquake engineering. 2008.
[19] Pinto PE, Giannini R, Franchin P. Seismic reliability analysis of structures. Pavia (Italy): IUSS Press; 2004.
[20] Mucciarelli M, Spinelli A, Pacor F. Un programma per la generazione di accelerogrammi sintetici fisici adeguati alla nuova normativa. In: XI *Convegno ANIDIS*, *''L'Ingegneria Sismica in Italia''*. 2004.
[21] Sabetta F, Pugliese A. Estimation of response spectra and simulation of non stationary earthquake ground motions. Bull Seismol Soc Am 1996;86(2): 337–52.
[22] Gasparini DA, Vanmarke EH. Simulated earthquake motions compatible with prescribed response spectra. MIT civil engineering research report R76-4. Cambridge (MA): Massachusetts Institute of Technology; 1976.
[23] Cosenza E, Manfredi G, Ramasco R. The use of damage functionals in earthquake-resistant design: a comparison among different procedures. Earthq Eng Struct Dyn 1993;22(10):855–68.
[24] Iervolino I, Giorgio M, Galasso C, Manfredi G. Prediction relationships for a vector valued ground motion intensity measure accounting for cumulative damage potential. In: 14th world conference on earthquake engineering. 2008.
[25] Iervolino I, Galasso C, Manfredi G. Conditional hazard analysis for secondary intensity measures. Bull Seismol Soc Am 2009 (submitted for publication).
[26] Clough RW, Johnston SB. Effect of stiffness degradation on earthquake ductility requirements. In: Proceedings of Japan earthquake engineering symposium. 1966.
[27] Takeda T, Sozen MA, Nielsen NN. Reinforced concrete response to simulated earthquakes. J Struct Eng Div, ASCE 1970;96(12):2557–73.
[28] Bazzurro P, Luco N. Post-elastic response of structures to synthetic ground motions. Report for pacific earthquake engineering research (PEER) Center Lifelines Program Project 1G00 Addenda. CA (US); 2004.
[29] Benjamin J, Cornell A. Probability, statistics and decision for civil engineers. NY (USA): Mc Graw-Hill; 1970.
[30] Lilliefors HW. On the Komogorov–Smirnov test for normality with mean and variance unknown. J Am Statist Assoc 1967;62:399–402.
[31] Welch BL. The significance of the difference between two means when the population variances are unequal. Biometrika 1938;29:350–62.
[32] Satterthwaite FE. Synthesis of variance. Psychometrika 1941;6(5):309–16.